Interplay of latent heat and time-dependent nucleation effects following pulsed-laser melting of a thin silicon film

Vitaly A. Shneidman[a)]
Department of Materials Science and Engineering, The University of Arizona, Tucson, Arizona 85721

(Received 18 September 1995; accepted for publication 11 April 1996)

We propose a simple-form mathematical description that allows us to account simultaneously for the effects of time-dependent nucleation and of latent heat during rapid cooling of a thin film. The method is based on a combination of analytical description of nucleation and a numerical (or, semianalytical) description of thermal effects due to postnucleation growth of crystallites. The accuracy of the treatment is tested against numerically exact solutions of the Farkas–Becker–Döring master equation, and is applied to several realistic cooling histories consistent with experimental studies of silicon on silicon oxide films of Stiffler *et al.* [Phys. Rev. B **43**, 9851 (1991)] and Sameshima and Usui [J. Appl. Phys. **70**, 1281 (1991)], respectively. Special attention is paid to the region of high cooling rates (very thin films of less than 100 nm) where the transition to complete amorphization occurs. For such cooling rates the time-dependent nucleation effects turn out to be especially important, and their neglect would lead to significant overestimates of the critical cooling rate that separates the recrystallization and the amorphization regions. © *1996 American Institute of Physics.* [S0021-8979(96)04814-1]

I. INTRODUCTION

Pulsed laser annealing of thin silicon films represents a powerful tool both for understanding fundamental properties of this element and for manipulating these properties on a microstructural level in view of applications in semiconductor devices.[1–9] Normally, the pulsed irradiation of a film leads to its partial melting and subsequent recrystallization;[1] partial amorphization of the melted fraction on the surface of bulk silicon also was observed in pico- [10] and nanosecond laser experiments.[11] On certain occasions, however, complete melting of the silicon film is achieved and is followed by a deep undercooling of the melt[3] with a possibility of its quenching into the amorphous state.[4] The two latter situations will be of primary interest for the present study.

Due to the very high cooling rates achieved after pulsed-laser irradiation (10^{10} K/s and more), the expected mechanism of phase transformation is homogeneous nucleation and growth of crystallites. The standard description of these two processes can be traced back to the works of Volmer and Weber, Farkas, Becker and Döring, Zeldovich, and Frenkel[12] (nucleation) and by Kolmogorov, Johnson and Mehl, and Avrami[13] (postnucleation growth and interaction between crystallites), respectively. Both descriptions[12] and[13] involve an essential assumption that the nucleation rate is a function of the current state of the system and does not depend on the cooling rate [for that reason we henceforth label this description as the quasi-steady-state (QSS) approximation]. One can show that the other assumption, the one of size-independent growth,[13] is valid under the same conditions as the QSS nucleation rate. The standard approach, thus, is very well balanced in its basic approximations and, generally speaking, gives an accurate description of the crystallized volume fraction. It turns out, however, that due to the above mentioned high values of the cooling rate (and due to specific values of physical parameters of silicon) the QSS approximation can lose its accuracy when the crystallized fraction is evaluated in very thin films and, on certain special occasions, can lead even to qualitatively incorrect results when the final state of the film is predicted. The possibility of non-QSS nucleation effects in pulsed-laser melted silicon films was first indicated in connection with the experimental study,[3] and subsequent numerical analysis[14] confirmed the potential failure of the QSS approximation when evaluating the limits of undercooling in such systems.

Numerical solutions of the time-dependent version of the nucleation master equation (due to Farkas, and Becker and Döring) and of the equations for postnucleation growth of crystallites provide a powerful tool in the description of the phase transformation kinetics in situations when the QSS approximation is invalid. Under the conditions of continuous cooling, the numerical approach was introduced by Kelton and Greer[15] to describe the formation of lithium disilicate and several metallic glasses and, without taking account of latent heat effects (small volume fractions of the crystalline phase) a similar approach was applied to melted silicon films by Evans and Stiffler.[14] In a sense, the numerical description is more accurate than any analytical approximation, and below we will often refer to it as to ''numerically exact.'' Nevertheless, even this approach can have its limitations in complicated (spatially inhomogeneous) systems that already require extensive computational effort to describe heat conductivity, melt flow, etc. A reasonably accurate analytical approximation in description of nucleation and growth can, thus, deserve consideration not only from a purely academic point, but also in applications.

In the analytical description one can distinguish between the isothermal (transient) formulation of the general problem of time-dependent nucleation and its nonisothermal formulation, which is more relevant to the experimental situations discussed. The method of solution of the nucleation equation in both formulations is based on the matched asymptotic

a)Electronic mail: vitaly@louie.aml.arizona.edu

 0021-8979/96/80(2)/803/9/$10.00

(singular perturbation) approach[16] that employs large values of the nucleation barrier, W_*, compared to the thermal energy, kT. The difference, however, comes at the growth stage. In the isothermal case the growth equations can be solved exactly, which allows one a direct extension of the nucleation solution up to an arbitrary size in the growth region.[17] In the nonisothermal situation, in a general case the growth equations cannot be solved exactly *in principle*. For that reason inclusion of growth in the nucleation solution in the nonisothermal case inevitably involves additional approximations and requires as much analytical effort as the solution of the nucleation equation itself.[18] Fortunately, the final analytical result (which is described below) turns out to be an elementary function that compared to the QSS expression[12] contains only one additional parameter, the dimensionless rate of the barrier change. Thus, the non-QSS analytical description can be represented in the same standard form as the familiar QSS approximation with only minor modification of the coefficients.

With respect to applications, an account of nucleation and growth is only the starting point of the description of the phase transformation. One still has to consider latent heat released in the course of crystallization[19] that, in turn, affects both nucleation and growth. For a realistic setting of the problem such nonlinear effects hardly can be described analytically in a reasonably simple manner. On the other hand, since the analytical results on nucleation and growth in any case are to be placed into the numerical description of thermal effects, one can seek for the most ''convenient'' (for applications) semianalytical representation of the analytical expressions. The latter represents one of the key points of the present study, leading to a method that potentially combines the advantages of both analytical and numerical approaches, i.e., the simplicity of the former and the accuracy of the latter. For a simpler, spatially homogeneous situation (which nevertheless is expected to imitate realistically the experimental setting of Ref. 3), the method will be tested against a numerically exact description with latent heat effects included. The description will be used to gain quantitative understanding of the interplay of non-QSS nucleation effects and the effects of latent heat for cooling rates close the critical cooling rate, S^*, which separates the cases of recrystallization and amorphization.

The paper is organized in the following manner:

In Sec. II the standard QSS approximation for nucleation and growth is introduced, and the non-QSS corrections are considered. Selection of the nucleation-growth model is also discussed here.

In Sec. III thermal effects are examined. A closed system of equations that allows us to combine in a simple manner the non-QSS nucleation effects with those due to latent heat released in the course of crystallization, is introduced in Sec. III A. In Sec. III B the heat conductivity problem is considered for two specific settings that are related to experimental studies of Refs. 3 and 4, respectively, and simple relations between the film/insulator thickness and the cooling rate are established. A criterion of spatial homogeneity of nucleation, which allows an essential simplification of the general description is also discussed.

In Sec. IV A the physical parameters in the proposed semianalytical description are adjusted for experimental data of Ref. 3. In Sec. IV B this description is used to evaluate the crystallized volume fraction for different values of the cooling rate and to calculate the critical cooling rate, S^*. Under identical conditions the numerical and the QSS approaches are applied as well. This allows us to estimate the accuracy of the proposed semianalytical description and to elucidate the limitations of the QSS approximation. The predicted values of S^* are used to assess the critical film thickness h in the experimental setting close to the one of Ref. 4 and to compare it to the values measured in that study.

Section V contains the discussion.

II. BACKGROUND

A. Nucleation and growth: selection of the model

The classical treatment[12] describes nucleation as a random walk of a nucleus in the space of its ''sizes'' (cluster numbers, g). Evolution with time of the cluster distribution function $f_g(t)$ can be described by a master equation, which according to Farkas, and Becker and Döring[12] can be written as

$$\partial f_g/\partial t = j_g - j_{g+1}, \quad j_g = \beta_{g-1} f_{g-1} - \alpha_g f_g, \tag{1}$$

with α_g and β_g being the kinetic loss and gain coefficients, respectively. The principle of detailed balance allows one to relate the two groups of kinetic coefficients via the quasi-equilibrium distribution, f_g^{eq}, which corresponds to a zero flux, j_g. From general thermodynamic considerations it can be estimated as

$$f_g^{\mathrm{eq}} \approx f_1 \exp\{-W(g)/kT\}, \tag{2}$$

with f_1 being the number of monomers in the system and $W(g)$ the minimal work required to form a nucleus with a given cluster number. In the classical description[12] this work has the form

$$W(g) = -g\,\delta\mu + 4\pi R^2 \sigma, \quad R \equiv (3Vg/4\pi)^{1/3}, \tag{3}$$

where $\delta\mu$ is the difference of chemical potentials, σ the interfacial tension, R the radius of a spherical cluster, and V is the molecular volume of the solid phase. At the critical radius, $R_* = 2\sigma V/\delta\mu$, Eq. (3) has a maximum, $W_* \equiv W(R_*)$, which represents the barrier to nucleation.

The specification of a kinetic model comes through a particular selection of the size and temperature dependence of the kinetic coefficients β_g in Eq. (1). The size-dependence $\beta_g \propto g^{2/3}$ was originally discussed by Farkas, and Becker and Döring[12] in terms of vapor condensation. In solid-state nucleation the most frequently used is the Turnbull–Fisher (TF) model[20] with

$$\beta_g \sim g^{2/3} \exp\{[W(g) - W(g+1)]/2kT\}. \tag{4}$$

In the steady-state case predictions of all models for the nucleation flux, $j_g = \mathrm{const} \equiv I_{\mathrm{st}}$ are asymptotically identical in the limit of a high barrier $W_* \gg kT$. This flux (per monomer of the metastable phase) is given by[12]

$$I_{st} \approx \frac{\Delta}{2\tau\sqrt{\pi}} \exp\left(-\frac{W_*}{kT}\right), \tag{5}$$

with

$$\tau = \frac{\Delta^2}{2\beta(g_*)}, \quad \Delta^{-2} = -\frac{1}{2kT}\left.\frac{\partial^2 W}{\partial g^2}\right|_*. \tag{6}$$

In contrast, in the time-dependent situation and when describing postnucleation growth (see below) the differences between models can become important. From the experimental point of view, however, different models are very hard to distinguish and, qualitatively at least, the results are expected to be more general than the specific TF model employed.

The treatment of postnucleation growth requires a knowledge of the deterministic growth rate, $\dot{R}$. Correspondence with the nucleation description dictates the form of $\dot{R}(R) \simeq dR/dg(\beta_g - \alpha_g)$, which in the TF case leads to[15]

$$\dot{R} \simeq \frac{2kTR_*}{\delta\mu\tau} \sinh\left[\frac{\delta\mu}{2kT}\left(1 - \frac{R_*}{R}\right)\right]. \tag{7}$$

In the following study we expect that Eq. (7) is valid for sizes large enough to give the main contribution to the crystallized volume fraction and that these sizes are still smaller than the film thickness (otherwise, the type of growth will change[8,21]). The growth rate of large crystallites can, thus, be determined as

$$u \equiv \dot{R}(\infty) = 2kTR_*/(\delta\mu\tau)\sinh[\delta\mu/2kT]. \tag{8}$$

With respect to the temperature dependence of the kinetic coefficient β_g (or, equivalently of the time scale τ), two alternative approaches are possible. The first one relates β_g to microscopic characteristics of the metastable phase, as was discussed for the solid-phase nucleation by Turnbull and Fisher. The second approach, which was originally introduced by Zeldovich to describe cavitation in a viscous fluid,[12] starts with a macroscopic (hydrodynamic) description of growth $\dot{R}(R)$. In principle, this allows one to obtain the time scale τ as the inverse of $d\dot{R}/dR$ at $R = R_*$ and, hence, to reconstruct the temperature dependence of β_g using Eq. (6). Although no hydrodynamic-type description of growth of a crystallite from a melt is currently available, it seems very likely (and is generally accepted[22,23]) that for strongly undercooled melts the growth rate should be limited by the viscosity, η. If, in addition, one takes into account the conditions $u \propto \delta\mu$ for $\delta\mu \to 0$, and assumes insensitivity of τ to the surface tension, then, just from the dimensional considerations, one obtains

$$\tau \propto \frac{\eta V kT}{(\delta\mu)^2}. \tag{9}$$

The same time scale τ turns out to be responsible for transient nucleation effects as well (see next section); in this sense the temperature part of Eq. (9) is consistent with the one proposed in Ref. 24. The temperature dependence of the viscosity is usually described as

$$\ln \eta = A + B/(T - T_0), \tag{10}$$

where A, B, and T_0 are empirical coefficients known as the ''Fulcher parameters.'' The proportionality coefficient in Eq. (9) cannot be specified until a consistent hydrodynamic theory of growth is constructed, but it always can be corrected by adjustment of the parameter A in the Fulcher expression.

After all kinetic parameters of growth are specified, one can describe the evolution of the distribution function $f(R,t) \equiv f_g(t)dg/dR$ using a continuity equation

$$\frac{\partial f}{\partial t} + \frac{\partial}{\partial R}(\dot{R}f) = 0. \tag{11}$$

The ''nucleation rate,'' I, enters this expression via the left-hand boundary condition $\dot{R}f(R,t) = I$ at some postcritical size $R = R_0$. This just means that crystallites are ''injected'' into the growth region with a rate I and with initial size R_0. The value of I can be associated with the flux j_g at $g = g_0 \equiv 4\pi R_0^3/3V$. The size R_0 that marks the transition from random nucleation to deterministic growth is an auxiliary parameter and must not affect the results in a consistent treatment. This insensitivity is of asymptotic nature and originates from large values of the reduced barrier W_*/kT (otherwise, separation of the nucleation and growth regions is impossible). In the analytical expressions that we present below, matching of the nucleation and growth regions is completed, and these expressions are, thus, explicitly independent of R_0. On the other hand, in numerical descriptions a choice of R_0 is inevitable and, similarly to Refs. 15 and 25, several different values will be considered in order to test the aforementioned insensitivity.

B. Time-dependent effects

One can show[16] that in the absence of a quench, i.e., in the isothermal case, establishment of the steady-state nucleation rate can be characterized by two time scales, τ and $\tau \ln(W_*/kT)$ (''relaxation'' and ''incubation'' times, respectively), with τ defined in Eqs. (5) and (6). [An explicit expression for the time dependence of the isothermal (transient) flux is also available[16,17] although it is less relevant to the situation discussed].

In view of the crucial importance of the reduced barrier, W_*/kT, in the nucleation problem one can expect that in a general nonisothermal situation deviation of the nucleation flux I from I_{st} will be mainly determined by the dimensionless rate of the barrier change on the scale of τ. In other words, the ''nonstationary parameter''[16]

$$n = -\tau \frac{\partial}{\partial t}\frac{W_*}{kT} \tag{12}$$

is expected to be responsible for non-QSS nucleation effects. The presence of the second, larger time scale implies that the non-QSS effects become strong already for moderate values of $n \sim 1$. An n- (and g_0) dependent expression for the nucleation flux is given by Eq. (20) (Ref. 16). Remarkably, the same parameter n also turns out crucial in the description of postnucleation growth.[18] Due to the rapid increase of the growth rate u with temperature, the size of a crystallite by

the end of the quench, $\overline{R}$, is mainly determined by the instant when this crystallite was nucleated, which gives[18]

$$\overline{R} \approx \frac{4R_*}{n(T)}. \tag{13}$$

This allows one to extend the nucleation solution into the growth region, and to introduce an ''effective nucleation rate,'' which accounts for both non-QSS nucleation effects and for size-dependent effects in post-nucleation growth[18]

$$I^{\text{eff}} \simeq I_{\text{st}} \left(\frac{W_*}{nkT} \right)^{-n}. \tag{14}$$

In contrast to the steady-state expression, Eq. (5), the effective nucleation rate does depend on the quench rate via the dimensionless parameter n. The deviation of I^{eff} from I_{st} can be substantial even for small values of n due to the presence of the large parameter W_*/kT. Rigorously speaking, Eq. (14) is expected to be accurate only for $n<1$, but in practice, in the spirit of asymptotic expansions, it can be used until the correction decays with n, i.e., for $n<W_*/(ekT)$ ($e=2.718...$). For larger values of n the time-dependent effects dramatically suppress the nucleation rate and it can be set to zero. Note that the effective nucleation rate I^{eff} (in contrast to the flux j_g) does not depend on size. This signifies that matching with the growth region has already been performed and subsequent growth can be described as size independent (i.e., $\dot{R} \simeq u$). As will be discussed below, the latter circumstance allows an essential simplification of the solution of the continuity Eq. (11) and the description of the entire phase transformation process.

III. THERMAL EFFECTS

A. Heat released from nucleation and growth

For a large number of finely dispersed crystallites one can describe the coarse-grained temperature distribution by a standard heat conductivity equation with a distributed heat source, Q (Ref. 26)

$$C_p \dot{T}(\mathbf{r},t) = \boldsymbol{\nabla}(\kappa \nabla T) + Q(\mathbf{r},t). \tag{15}$$

(C_p is the specific heat and κ the heat conductivity coefficient). The intensity of the heat source is determined by the latent heat released during growth and is given by

$$Q = L\dot{x}. \tag{16}$$

Here L is the latent heat of fusion ($\approx$4200 J/cm^3 for silicon) and x is the crystallized volume fraction, which for small values discussed in the present study just corresponds to $\Omega_3(\mathbf{r},t)$, the third moment of the distribution $f(R,t,\mathbf{r})$

$$x \simeq (4\pi/3V)\Omega_3. \tag{17}$$

There exist two possibilities of evaluation of Ω_3 and its derivatives that give the intensity of the heat source, Q.

The first method, the ''numerically exact'' one, requires a direct solution of Eqs. (1) and (11). In this case, evaluation of the distribution of large particles allows one to calculate the moments of this distribution and their increments. In its main features this method corresponds to the one of Refs. 14, 15, and 25. Adding the latent heat effects just effectively changes the cooling rate, $-dT/dt$. [For strong heat release effects cooling can be replaced by heating (see below), but this does not lead to any essential modification of the computations.] Adding the space dependence of the distribution increases the computational time, but, in principle, should not lead to any dramatic complications as long as diffusion of nuclei in the $\mathbf{r}$ space is neglected.

The second, semianalytical approach that is of primary interest for the present study, is based on Eq. (14) for the effective nucleation rate. When describing further growth of nucleated particles this equation allows one to treat the growth rate $\dot{R}$ as size independent (i.e., replace $\dot{R}(R)$ by u). In this case the continuity Eq. (11) can be replaced by a simple set of *ordinary* differential equations for its lower moments, Ω_i

$$\frac{d\Omega_i}{dt} = iu\Omega_{i-1}, \quad i=1,2,3, \tag{18}$$

$$\frac{d\Omega_0}{dt} = I^{\text{eff}}(T,n). \tag{19}$$

A similar form of the equations with I^{eff} replaced by I_{st} (which corresponds to the QSS approximation) is familiar in vapor condensation problems.[27] The major novelty of the present study is the incorporation of time-dependent nucleation effects and the effects of size-dependent growth via the nucleation rate $I^{\text{eff}}(T,n)$ without otherwise altering the convenient *form* of the QSS description. In the specific application of Eqs. (18) and (19) to thin films, an additional requirement $\Omega_i/\Omega_{i-1} \ll h$ should be satisfied, implying that the characteristic size of the particles is much smaller than the film thickness, h.

As mentioned, strong latent heat effects can reverse the sign of the cooling rate, leading to negative values of the parameter n. In this case Eq. (14), which was obtained specifically for cooling ($n>0$), becomes inapplicable, but one can show that the number of crystallites nucleated during heating ($n<0$) is negligible compared to the cooling stage nucleation. Thus, one can either completely neglect nucleation on the heating stage, i.e., put $I^{\text{eff}} \equiv 0$ for $n<0$ or, in order to keep the expression continuous, use for $n<0$ the QSS approximation $I^{\text{eff}} = I_{\text{st}}$ (the latter will be mostly employed in the forthcoming calculations). The insensitivity of the physical results to the specific choice of I^{eff} at $n<0$ (which is tested in numerical simulations) is the best indicator that nucleation effects on the heating stage are already minor and only growth of previously nucleated crystallites is important.

The system of Eq. (14)–(19), together with the boundary conditions for the temperature on the surface of the sample, provides a closed description of time-dependent nucleation with thermal effects. In the next section a simple setting of the heat conductivity problem that allows one to eliminate the dependence on space variables will be considered. This will permit a simultaneous application of both the more accurate ''numerically exact'' and the semianalytical approaches, thus providing a crucial test for the latter and permitting its potential use in more complicated situations.

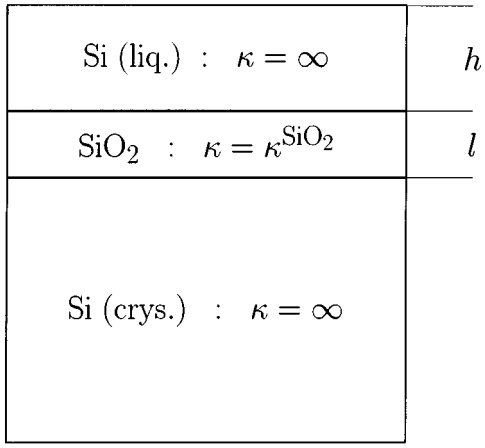

(a)

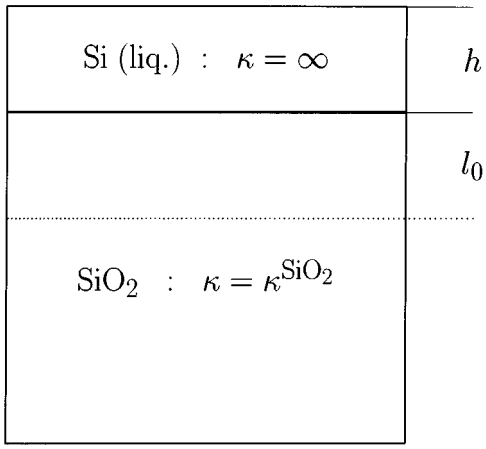

(b)

FIG. 1. Two settings of the heat conductivity problem and approximations used in the analytical treatment. (a) ''Thin insulator limit.'' (b) ''Thick insulator limit.'' The heated layer, l_0, is due to the heat leakage into the substrate during laser melting. At $t=0$ (immediately after melting) the temperature inside this layer is expected to coincide with the melting temperature of silicon, T_m.

B. Two simplified models of experimental situations

In experimental studies a silicon film that was previously melted by a laser pulse is rapidly cooled due to heat leakage into the substrate. The substrate (crystalline Si) is separated from the film by a thin layer of SiO_2 (Ref. 3) or, alternatively; the substrate itself can be composed of quartz,[4] see Figs. 1(a) and 1(b), respectively (we are discussing only experiments where complete melting was achieved). The heat conductivity of the insulator, κ^{SiO_2}, is substantially smaller than that of liquid silicon [about 70 times (see, e.g., Table I in Ref. 6)]. This allows one to approximate the silicon film as a system with an infinite heat conductivity (limitations of this approximation will be evaluated below later). Further simplification is achieved when only two limiting cases of ''thin'' and ''thick'' insulators are considered, as in Fig. 1. Radiative cooling from the surface is neglected. The two simple models are not intended in any way to replace the full solution of the nonstationary heat conductivity problem (which in a general case requires a nontrivial combination of experimental and numerical methods[3,5,6,11,19]). Rather, the intent of these models is to ''mimic'' the realistic values of cooling rates achieved in experiments (see below), thus providing a qualitatively correct basis for investigation of latent heat and nucleation effects.

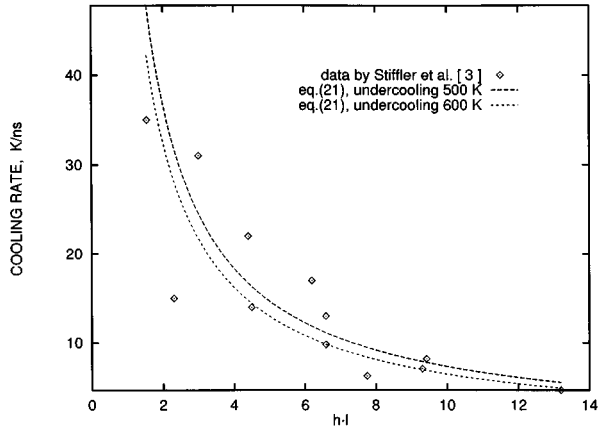

FIG. 2. Cooling rate in the model setting of Fig. 1(a) as a function of the product of the thicknesses (in 10^{-10} cm^2) of the film (h) and the insulator (l).

Let us first consider case I [Fig. 1(a)]. The temperature and other variables are uniform across the Si film in the limit of infinite conductivity, and the cooling rate is determined by the balance of the rates of the heat leakage, q, in the substrate and the rate of latent heat release, Qh with h being the thickness of the Si film. For the heat leakage one has

$$q=\kappa^{SiO_2}(T-T_r)/l, \tag{20}$$

with l being the thickness of the SiO_2 film, $\kappa^{SiO_2} \simeq 0.02$ J/(cm s K) heat conductivity of quartz,[6] and $T_r \simeq 300$ K ''room temperature'' (the temperature of the silicon substrate). One, thus, obtains for the cooling rate

$$-\dot{T}=\frac{\kappa^{SiO_2}}{C_p^{Si}}\frac{T-T_r}{hl}-\frac{Q}{C_p^{Si}}, \tag{21}$$

with $C_p^{Si} \approx 2.6+3\times10^{-4}(T-T_m)$ J/cm^3 K being the specific heat of melted silicon. The heat capacity of the SiO_2 film in this approximation is neglected, which implies $l<h$.

Numerical values of the cooling rates predicted by Eq. (21) before the onset of intensive nucleation and growth (i.e., with $Q=0$) are shown in Fig. 2 for two different values of the undercooling T_m-T ($T_m=1685$ K is the melting temperature). This figure also contains the cooling rate data reported in Table I of Ref. 3 for the same values of h and l. The scatter of experimental points is partly due to the crudeness of the present model used for their presentation in Fig. 2. In reality, the product hl is not the only parameter that affects the cooling rate [particularly, taking into account the finite heat capacity of the SiO_2 film by replacing h in Eq. (21) by $h+lC_p^{SiO_2}/2C_p^{Si}$ could reduce the scatter]. Nevertheless, since no matching parameters were used in Fig. 2, the model at least can be considered reasonable when describing the cooling history.

The assumption of spatial homogeneity of variables inside the silicon film becomes most vulnerable when applied to the nucleation rate, which is extremely sensitive to temperature. The temperature gradient inside the film can be estimated as $(\kappa^{SiO_2}/\kappa^{Si})(T - T_r)/l$, and the derivative of the nucleation barrier is estimated as $\partial(W_*/kT)/\partial T \sim 2(W_*/kT)/(T_m - T)$. This gives the condition that allows one to treat the nucleation rate as homogeneous

$$\frac{2W_*}{kT}\left[\frac{\kappa^{SiO_2}}{\kappa^{Si}}\frac{h}{l}\frac{T-T_r}{T_m-T}\right] \ll 1. \tag{22}$$

Actually, this condition is close to violation in the experimental situation discussed: Although the term in square brackets in Eq. (22) is small (which just means small values of the thermal gradient; see also numerical estimations in Refs. 5 and 14), the remaining factor $2W_*/kT$ is large enough to make the nucleation rate change noticeably across the film. In what follows, nucleation will still be treated as spatially homogeneous. This is mostly due to our intent to test the analytical approximation against the numerically exact description, which technically is much harder to obtain in the inhomogeneous case. However, one can expect that as long as only *small* values of the crystallized volume fraction are discussed (i.e., no such specifically inhomogeneous effects as formation of a crystallization front are encountered), the ''homogeneous'' approximation for nucleation remains reasonable at least on a qualitative level.

Consider now case II, which is the ''thick insulator limit'' [Fig. 2(b)]. Here the heat conductivity problem turns out to be much more sensitive to initial conditions, which are determined by heat leakage *during* the pulsed-laser heating. To imitate this effect we introduce a heated layer with a thickness l_0 at the beginning of cooling. The thickness can be estimated from the assumption that during a fraction $\alpha < 1$ of the heating period the boundary of the insulator had the temperature of melted silicon, T_m (the values of α can be adjusted to describe a more realistic heating history). The temperature of the heated layer upon completion of heating after the time t_h ($t_h \simeq 30$ ns) Ref. 4 in this case is close to T_m and its width can be estimated as[26] $l_0 \simeq (4\alpha\kappa^{SiO_2}t_h/C_p^{SiO_2})^{1/2}$. The solution of the corresponding heat-conductivity problem is readily obtained by the Laplace transformation method. After certain transformations one obtains for the temperature of the silicon film

$$\frac{T-T_r}{T_m-T_r} \equiv \xi(z) = \mathrm{erf}\,\frac{a}{\sqrt{z}} + \exp(2a+z)\,\mathrm{erfc}\left(\sqrt{z}+\frac{a}{\sqrt{z}}\right), \tag{23}$$

with

$$a = \frac{l_0}{2h}\frac{C_p^{SiO_2}}{C_p^{Si}}, \quad z = \frac{\kappa^{SiO_2}C_p^{SiO_2}}{h^2(C_p^{Si})^2}\,t. \tag{24}$$

The cooling rate is given by

$$\dot{T} = (T_m - T_r)\,\frac{\kappa^{SiO_2}C_p^{SiO_2}}{h^2(C_p^{Si})^2}\,\frac{d\xi}{dz}. \tag{25}$$

Note that despite the seemingly unlimited increase of the cooling rate [Eq. (25)] in the limit $h \to 0$, this cooling rate is bounded in the case of finite heat leakage ($\alpha > 0$) due to the increase in the relative thickness of the heated layer, a. In fact, for $h \to 0$ ($a \to \infty$) the second term in Eq. (24) can be neglected and the temperature of 1100 K is achieved at $a/\sqrt{z} \simeq 0.57$. For the cooling rate one, thus, obtains an h-independent expression

$$-\dot{T} \sim \frac{3\times 10^9}{\alpha}\ \text{K/s}. \tag{26}$$

In Sec. IV we will show that the critical cooling rate is close to 10^{11} K/s, which means that in the thick-insulator limit it can be achieved only for extremely small heat leakage α, not more than several percent.

IV. ILLUSTRATIVE RESULTS

Due to the abundance of unknown parameters in the nucleation and growth formulas it is hard to imagine a set of experimental data that could not be matched by a given analytical expression. For a meaningful comparison, however, one could still attempt to (a) minimize the number of matching parameters used to describe a chosen set of data and (b) use the predictions for comparison with data of different experiments (with no matching parameters used at that point). This at least will give a feeling of the possible error and, thus, of the degree of reliability of the general conclusions. As mentioned, the goal of the present study is *not* an accurate evaluation of the physical parameters of undercooled silicon, but rather, their realistic estimation, which would allow one to discuss latent heat vs time-dependent nucleation effects. Another goal that could be achieved here is to test the consistency of experimental studies of recrystallization[3] with those of complete amorphization.[4] Note, however, that the present treatment does not distinguish between the ''amorphous'' and the ''supercooled liquid'' states (which may differ from the experimental point of view[2]), and the results related to temperatures under 1000 K should be taken with certain caution.

A. Identification of nucleation and growth parameters

Consider first the ''thin-insulator'' cooling history described by Eq. (21). Using either the numerically exact or the analytical description of nucleation combined with numerical description of thermal effects, as described in Sec. III, one obtains the crystallized volume fraction as a function of temperature for different cooling rates (equivalently, for different values of the product of the silicon film and the insulator thicknesses $h \cdot l$). This is depicted in Fig. 3. The meaning of the plotted curves will be discussed in Sec. IV. B, but at the moment we note that the predicted undercoolings can be identified with the experimental data of Ref. 3 in order to obtain the values of unknown parameters. The parameters that were *not* adjusted in comparison with experimental data were those related to the temperature dependence and absolute values of the nucleation barrier and to the temperature dependence of the viscosity. These parameters were taken the same as in Refs. 3 and 14, respectively (e.g., the values

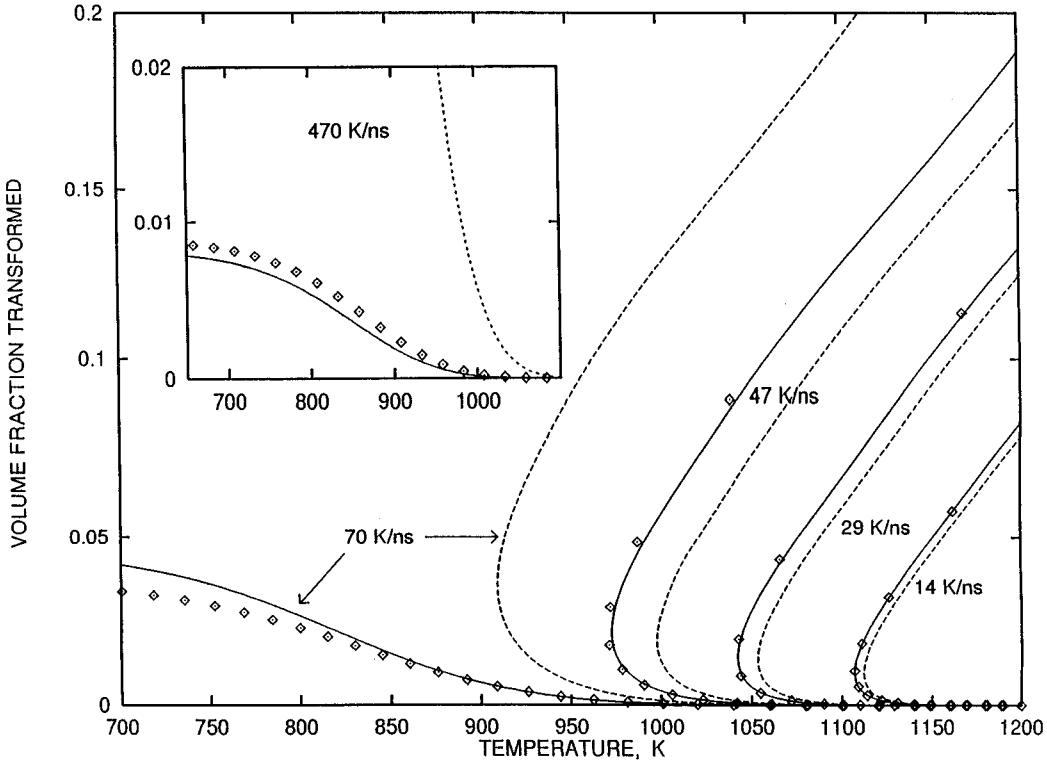

FIG. 3. Crystallized volume fraction for different quench rates. Solid lines, Eqs. (18) and (19); diamonds, numerically exact description of nucleation and growth; dashed lines, the QSS approximation. [For thermal effects in all three cases Eqs. (16) and (21) were employed.] The volume fraction for very fast quenches (the inset) is multiplied by 10^4; the QSS approximation, which is shown only partly for $S=470$ K/ns saturates at $x\approx 2.5\times 10^{-5}$.

$B=11\,590$ K and $T_0=0$ K were taken for the Fulcher parameters). The proportionality coefficient in Eq. (9) that relates the time scale τ to viscosity was taken as 16. The only parameter used for matching was the absolute value of the viscosity, described by the first Fulcher parameter, A. This parameter was adjusted to obtain an undercooling of 570 K at a cooling rate of 14 K/ns,[3] giving $A=-12.6$ when the viscosity is measured in cgs units (upon this choice other data of Ref. 3 are also fitted with reasonable accuracy, but this is more due to the successful choice of the activation energy, B, in Ref. 14).

Unfortunately, there are no measurements of viscosity and/or the growth rates at such high undercoolings that could provide an independent test of the chosen numbers. Nevertheless, extrapolating the analytic expressions close to the melting temperature one can compare the viscosity with the measurements reported *above* T_m (Ref. 28) (there seems to be no reason to expect a discontinuity in η when crossing T_m). The measured values ($\sim 10^{-2}$ g/cm s) are about three times larger, but this is a tolerable error since the values of η increase almost by two orders of magnitude between T_m and the nucleation temperature. The temperature derivative of the growth rate $u(T)$ at small undercoolings is about four times larger than the measured rate of the recrystallization front [$\sim$1/15 (m/s)/K (Ref. 3)]. Since the growth rate of an individual crystallite is the upper limit of the recrystallization rate,[29] and with the same arguments as used in the case of viscosity, the correspondence can be considered as acceptable at the moment.

Thus, we dare to conclude that the parameters that were obtained exclusively from the undercooling measurements of Ref. 3 at least do not contradict the high-temperature measurements, although additional study is required for more quantitative purposes. [Particularly, nonzero values of the Fulcher temperature, T_0 (with a corresponding modification of the parameter B) could be required to describe the low-temperature region].

B. Results

One can discuss two alternative situations that can take place during a rapid quench. In the case where the quench rate, S, is smaller than some critical value, S^*, the latent heat effects become sufficiently strong to reverse the sign of $\dot{T}$, leading to subsequent recrystallization of the film. For larger values of S the latent heat effects are too weak and the film becomes partly (or, completely, for very large S) amorphous due to small values of the crystallized volume fraction. The critical cooling rate corresponds approximately to the situation when the so-called ''nose temperature'' (i.e., the one corresponding to the maximum of $I_{st}(T)u(T)$[3,30] which is 988.8 K for the chosen parameters) is approached in the course of supercooling.

The two above mentioned alternatives are clearly seen from Fig. 3, where for the purpose of comparison all three methods of description are applied. The solid lines were produced using the semianalytical method given by Eqs. (18) and (19) (nucleation and growth) and Eqs. (16) and (21)

(thermal effects). Alternatively, Eq. (19) was replaced by $\Omega_0=I_{st}$, which corresponds to the QSS approximation (dashed lines). Finally, the numerically exact description of nucleation and growth based on Eqs. (1) and (11), respectively, was employed instead of Eqs. (18) and (19) (diamonds). The values of the cooling rate, S, which label each set of data in Fig. 3 were estimated around 1100 K (without latent heat effects for the slowest cooling).

As one can see from Fig. 3, the QSS approximation provides an accurate description only for sufficiently small values of S. Otherwise, it substantially overestimates the values of the volume fraction transformed and the amount of latent heat released. For that reason, in estimation of the critical rate, S^*, (which for the chosen parameters equals 66.5 K/s) the QSS approximation makes an error of more than 20%. There, thus, exists a certain region of S around the critical value where the QSS approximation is *qualitatively* incorrect, predicting complete recrystallization in situations where the film remains practically amorphous (as for 70 K/ns in Fig. 3). The inset of Fig. 3 shows the case of very high cooling rates so that ''complete amorphization'' [i.e., values of $\Omega_3<10^{-6}$ (Ref. 31)] is achieved. The QSS approximation overestimates here the volume fraction transformed by almost 30 times which, equivalently, implies about a 100% error in estimation of the cooling rate required for complete amorphization.

Predictions of the proposed semianalytical method, on the other hand, are rather close to numerically exact results. A minor difference at low temperatures is most likely due to the fact that the proposed analytical results are asymptotic, i.e., are accurate for sufficiently high values of the reduced nucleation barrier W_*/kT. At low temperatures these values are not excessively large (18.9 at the ''nose'' temperature), which limits the accuracy of the analytical description (although this accuracy remains more than sufficient in view of experimental uncertainties).

Consider now the second type of experimental setting with a ''thick'' insulator, as in Ref. 4. It was observed in these studies that amorphization is possible only for film thicknesses less than the ''critical value'' $h^*\sim 50$ nm. One could wish to test here that this value is consistent with the critical cooling rate of 66.5 K/s predicted by the non-QSS treatment with parameters based on the ''thin-insulator'' data of Ref. 3. Using Eqs. (23)–(25) with no heat leakage ($a=0$) one obtains the critical thickness as $h^*\sim 80$ nm. As mentioned, however, this result is extremely sensitive to the thermal state of the substrate. E.g., if only 1% of the irradiation time the temperature of the film–substrate boundary equals the melting temperature of silicon, T_m (i.e., $\alpha=0.01$), the critical thickness is reduced to about 35 nm, and for α exceeding several percent amorphization cannot be achieved at all. Unfortunately, there are insufficient data to estimate the heat leakage more definitely. Nevertheless, from the above numbers one still can conclude that in view of the non-QSS treatment the data of two very different experimental studies of Refs. 3 and 4 are at least not in contradiction with each other.

The value of S^* obtained is comparable with the values of 10^{11} K/s, which were mentioned in connection with pulsed-laser amorphization of the surface of *bulk* silicon.[11] However, quite similarly to the ''thick insulator'' situation discussed above, precise values of S are extremely sensitive to the thermal state of the substrate (unmelted silicon) right after the irradiation (see Fig. 1 in Ref. 11), which is not too well known, preventing a more quantitative comparison.

V. DISCUSSION

In the present study a semianalytical method to describe non-QSS nucleation and growth of crystallites in thin films was proposed. Accuracy of the method was tested against numerically exact data for the maximal undercoolings achieved for moderate cooling rates before recrystallization and for the amount of the crystalline phase trapped in the amorphous state for faster coolings (as well as for the values of the critical cooling rate S^*, which separates these two regimes). Although the test was performed for a relatively simple (spatially homogeneous) setting of the problem, there seems to be no reasons to expect the method to fail for more complicated situations (or, for different physical systems). The QSS approximation, on the other hand, is inaccurate for fast cooling rates (exceeding 10 K/ns in the case of silicon).

The proposed method can be directly generalized to describe nucleation and growth of crystallites in a flowing melt with a velocity field $\mathbf{v}(\mathbf{r})$. This is achieved by transition from local to full time-derivatives: $d/dt\rightarrow\partial/\partial t+\mathbf{v}\partial/\partial\mathbf{r}$ in Eqs. (18) and (19).

In view of the available experimental data, the non-QSS approach seems consistent (at least no contradictions were found) since it allows one to describe qualitatively different experiments (which lead either to amorphization or to recrystallization) without additional adjustment of parameters.

Normally, the non-QSS effects in nucleation are important only for very small values of the crystallized volume fraction, while the effects of latent heat are important when the volume fraction is sufficiently large. The possibility to observe these two effects simultaneously is rather unusual and is an additional reason to consider silicon as a remarkable element. The main reason for such an ''overlap'' of non-QSS and latent heat effects is due to moderate values of the reduced nucleation barrier, W_*/kT, which for deeply undercooled silicon is close to 20. Although the latter number should be considered tentative, one can expect that the situation is described qualitatively correctly since the ultimate limitation to observing the non-QSS nucleation effects is much higher [$W_*/kT\lesssim 30$ (Ref. 18)].

In view of potential applications it seems worth reiterating the role of the thermal state of the substrate immediately after irradiation (see also the discussion in Ref. 11). This effect is especially pronounced when the silicon film is placed directly on the substrate as in Fig. 1(b). E.g., preliminary cooling of the remote part of the substrate below room temperature could essentially facilitate achieving the critical cooling rate. The seemingly obvious reduction of the film thickness, on the other hand, has only a limited effect due to the relative increase of the heat leakage into the substrate during the laser pulse.

ACKNOWLEDGMENTS

The author is indebted to M. C. Weinberg for discussions and for comments on the manuscript, and to J. S. Im for drawing his attention to the existing pulsed-laser experiments.

[1] J. M. Poate and W. L. Brown, Phys. Today **35**, 24 (1982); also see A. Gat, L. Gerzberg, J. F. Gibbons, T. J. Magee, J. Peng, and J. D. Hong, Appl. Phys. Lett. **33**, 775 (1978); D. K. Biegelsen, N. M. Johnson, D. J. Bartelnic, and M. D. Moyer, Mater. Res. Symp. Proc. **1**, 487 (1981); G. J. Galvin, M. O. Thompson, J. W. Mayer, R. B. Hammond, N. Paulter, and P. S. Peercy, Phys. Rev. Lett. **48**, 33 (1981); G. J. Galvin, J. W. Mayer, and P. S. Peercy, Appl. Phys. Lett. **46**, 644 (1985); M. O. Thompson, Mater. Res. Soc. Symp. Proc. **100**, 525 (1988).
[2] J. A. Yater and M. O. Thompson, Phys. Rev. Lett. **63**, 2088 (1989).
[3] S. R. Stiffler, M. O. Thompson, and P. S. Peercy, Phys. Rev. B **43**, 9851 (1991).
[4] T. Sameshima and S. Usui, J. Appl. Phys. **70**, 1281 (1991); see also T. Sameshima, M. Hara, and S. Usui, Jpn. J. Appl. Phys. **29**, L548 (1990); T. Sameshima, M. Hara, N. Sano, and S. Usui, *ibid*. **29**, L1363 (1990).
[5] T. Sameshima and S. Usui, J. Appl. Phys. **74**, 6592 (1993).
[6] J. A. Kitt, R. Reitano, M. J. Aziz, D. P. Brunco, and M. O. Thompson, J. Appl. Phys. **73**, 3725 (1993).
[7] J. H. Shin and H. A. Atwater, Nucl. Instrum. Methods B **80/81**, 973 (1993).
[8] J. S. Im, H. J. Kim, and M. O. Thompson, Appl. Phys. Lett. **63**, 1969 (1993).
[9] N. Yamauchi and R. Reif, J. Appl. Phys. **75**, 3235 (1994).
[10] P. L. Lin, R. Yen, N. Bloembergen, and R. T. Hodgson, Appl. Phys. Lett. **34**, 864 (1979).
[11] R. Tsu, R. T. Hodgson, T. Y. Tan, and J. Baglin, Phys. Rev. Lett. **42**, 1356 (1979).
[12] M. Volmer and A. Weber, Z. Phys. Chem. **119**, 227 (1926); L. Farkas, *ibid*. **125**, 236 (1927); R. Becker and W. Döring, Ann. Phys. **24**, 719 (1935); Ya. B. Zeldovich, Acta Physicochim. USSR **18**, 1 (1943); J. Frenkel, *Kinetic Theory of Liquids* (Oxford University Press, Oxford, 1946).
[13] A. N. Kolmogorov, Bull. Acad. Sci. USSR (Sci. Mater. Nat.) **3**, 3551 (1937); W. A. Johnson and R. F. Mehl, Trans. AIME **135**, 416 (1939); M. Avrami, J. Chem. Phys. **7**, 1103 (1939); **8**, 212 (1940); **9**, 177 (1941).
[14] P. S. Evans and S. R. Stiffler, Acta Metall. Mater. **39**, 2727 (1991).
[15] K. F. Kelton and A. L. Greer, J. Non-Cryst. Solids **79**, 295 (1986).
[16] V. A. Shneidman, Sov. Phys. Tech. Phys. **32**, 76 (1987).
[17] V. A. Shneidman, Sov. Phys. Tech. Phys. **33**, 1338 (1988).
[18] V. A. Shneidman, J. Chem. Phys. **103**, 9772 (1995); Phys. Rev. Lett. **75**, 4634 (1995).
[19] R. F. Wood and G. E. Giles, Phys. Rev. B **23**, 2923 (1981).
[20] D. Turnbull and J. C. Fisher, J. Chem. Phys. **17**, 71 (1949).
[21] M. C. Weinberg, J. Non-Cryst. Solids **76**, 253 (1985).
[22] K. A. Jackson, D. R. Uhlmann, and J. D. Hunt, J. Cryst. Growth **1**, 1 (1967).
[23] D. Turnbull, Contemp. Phys. **10**, 473 (1969).
[24] C. V. Thompson, A. L. Greer, and F. Spaepen, Acta Metall. Mater. **31**, 883 (1983).
[25] K. F. Kelton, J. Non-Cryst. Solids **163**, 283 (1993).
[26] L. D. Landau and E. M. Lifshitz, *Fluid Mechanics* (Pergamon, New York, 1987).
[27] P. G. Hill, J. Fluid. Mech. **25**, 593 (1966).
[28] V. M. Glazov, S. N. Chizhevskaya, and N. N. Glagoleva, *Liquid Semiconductors* (Plenum, New York, 1969).
[29] F. Spaepen and D. Turnbull, AIP Conf. Proc. **50**, 73 (1979).
[30] M. C. Weinberg, B. J. Zelinski, D. R. Uhlmann, and E. D. Zanotto, J. Non-Cryst. Solids **123**, 90 (1990); M. C. Weinberg, *ibid*. **167**, 81 (1994).
[31] D. R. Uhlmann, J. Non-Cryst. Solids **25**, 73 (1977).